Amman, September 19, 2004
Note: **ME-1**

Mechanical Analysis of the Arc Vacuum Chamber Design (Rev. 0)

Maher M. Shehab

1.0 Introduction.

In this note we present a 3D model of the Arc Vacuum Chamber for the actual SESAME design [1÷3] together with a first 2D and 3D finite element evaluation of the mechanical deformation due to vacuum and self-weight load, with and without support system.

2.0 Geometrical Description and mechanical properties.

In Fig. 1 is shown the 3D drawing of the Arc Vacuum Chamber carried out with the CAD program Mechanical Desktop. The program was used to produce the 3D model of the chamber then IGES model was imported to ANSYS [4] workbench environment in order to mesh and to apply the required loads and material properties.

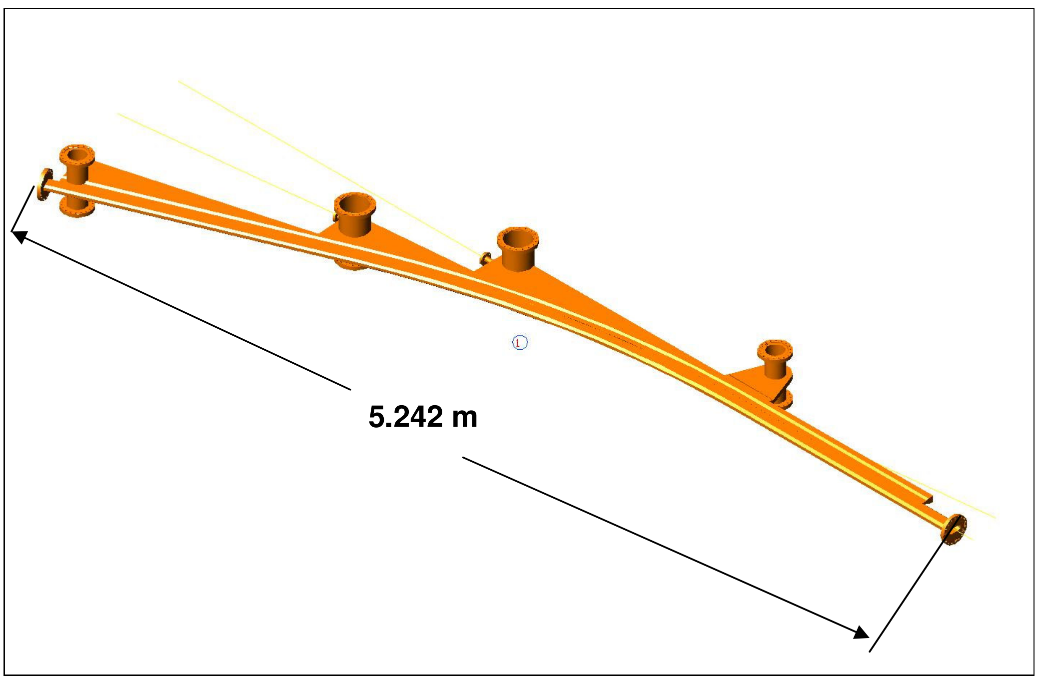

Figure 1: Arc Chamber 3D drawing.

The design of the stainless steel vacuum chamber is based on the chamber-antechamber concept, with OFHC crotch absorber. The required stay clear aperture in the chamber is 70mm in the horizontal plane and 30 mm in the vertical one. The chamber wall thickness is 3 mm, while the antechamber length in the transverse direction, depending on the position, is up to 25 cm.

The chamber material mechanical properties used in the analysis are listed in Tab. 1, while Fig. 2 shows a typical cross-section of the Vacuum Chamber inside the Dipole. Fig. 2 points out that *deformation* is one of the most critical design aspects of the vacuum chamber, since the *minimum clearance* inside the Dipole is only 1.224 mm.

Table 1: Stainless steel mechanical properties

Property	Value
Compressive Yield Strength	207.0 MPa
Density	7.75×10^{-6} kg/mm³
Poisson's Ratio	0.31
Tensile Yield Strength	207.0 MPa
Tensile Ultimate Strength	586.0 MPa
Young's Modulus	193,000.0 MPa
Thermal Expansion	1.7×10^{-5} 1/°C
Specific Heat	480.0 J/kg·°C

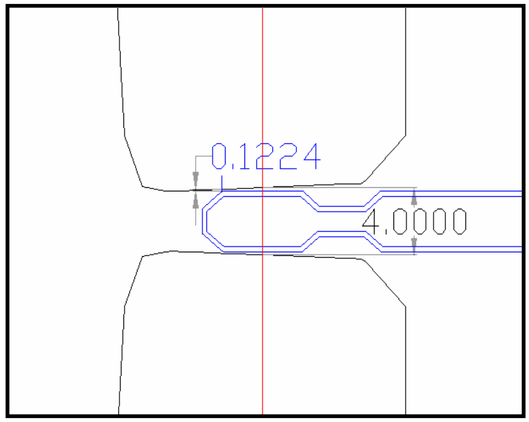

Figure 2: Minimum Clearance (cm) for the Vacuum Chamber inside the Dipole.

For completeness we summarize in Tab. 2 the minimum vacuum chamber clearance inside all the magnetic elements for half SESAME Superperiod.

Table 2. Minimum clearance for the vacuum chamber for half SESAME Superperiod

Magnetic Component	Critical Clearance Value & Location	Max Allowable Distance From Chamber Center	Current Distance From Chamber Center
Sextupole SF	1.1mm near slot zone	220 mm	38 mm
Quadrupole QF	2.4mm near slot zone	210 mm	38 mm
Quadrupole QD	2.4mm near slot zone	210 mm	38 mm
Sextupole SD	1.1mm near slot zone	220 mm	38 mm
Dipole	1.224mm Figure 2	N/A	N/A
Sextupole SD	1.1mm near slot zone	220 mm	112.054 mm
Quadrupole QD	2.4mm near slot zone	210 mm	137.881 mm
Quadrupole QF	2.4mm near slot zone	210 mm	174.2 mm
Sextupole SF	1.1mm near slot zone	220 mm	210.187 mm

3.0 Deformation Analysis.

Two load cases are considered separately in this study: vacuum-load and self-weight load. First we consider the vacuum-load effect only in a 2D geometry for different antechamber length and material thickness. Later we present the results in a 3D geometry of the deformation due to the self-weight load for different support arrangements.

3.1 2D Vacuum Loads vs. Anti-chamber length and Vacuum chamber wall thickness.

In Fig. 3 we plot the calculated 2D *Maximum deformation* and the *Deformation* at the critical zone inside the Dipole vs. the Anti-chamber length, while in Fig. 3÷6 the nodal solution output as given by ANSYS are shown for 4 different Anti-chamber lengths.

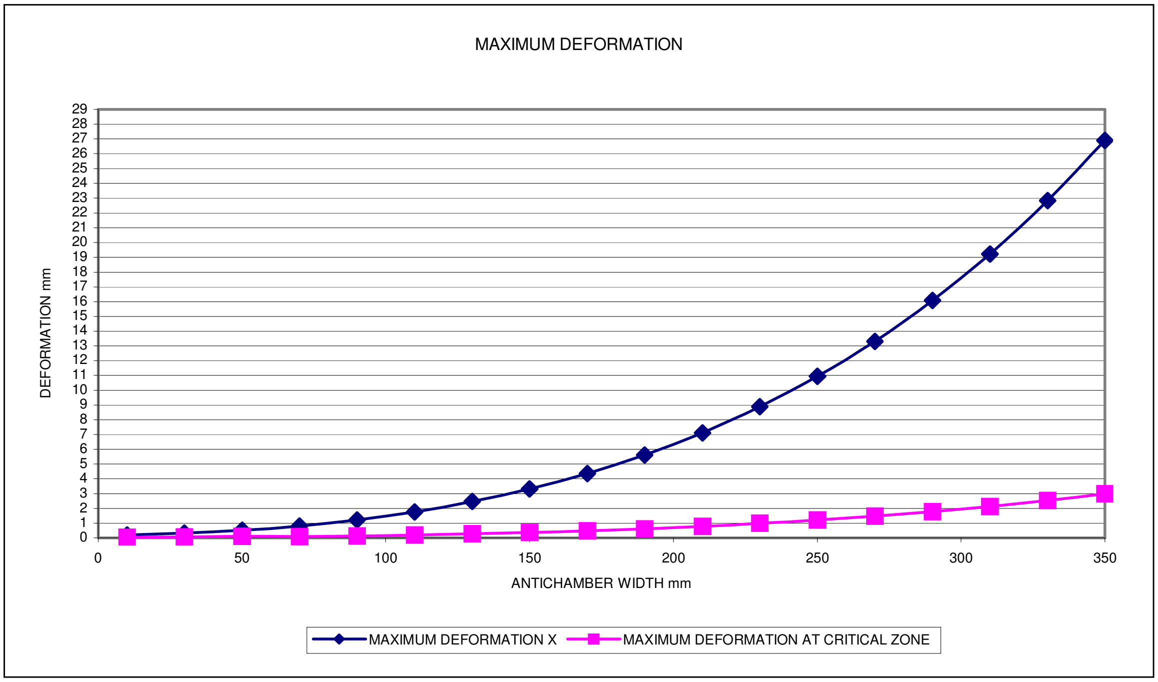

Figure 3: Maximum Deflection and Critical Deflection vs. Anti-chamber length.

It is clear that the absolute *Maximum deflection* and the *Critical* one are shifting toward the anti-chamber side as the anti chamber length increases.

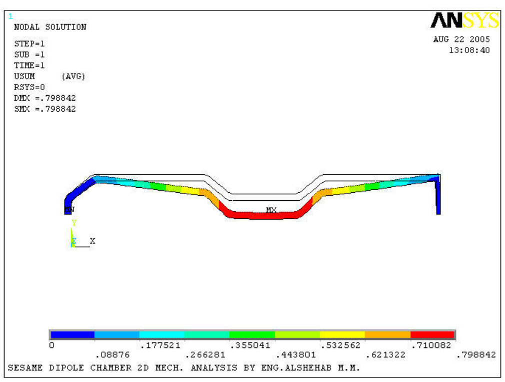

Figure 4: Deflection for 50mm anti-chamber width.

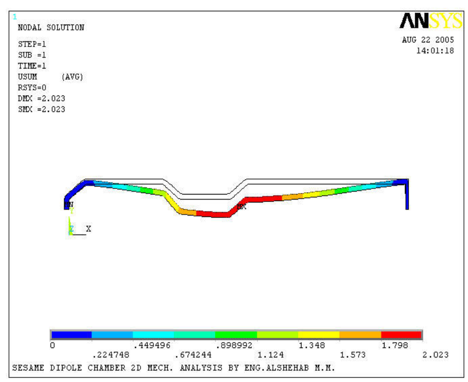

Figure 5: Deflection for 100mm anti-chamber width.

Finally, Fig. 8 shows the effect of the chamber wall thickness on the maximum deformation due to the vacuum load. It is very clear that decreasing the thickness will directly increase the maximum deformation, especially if the anti-chamber width increase.

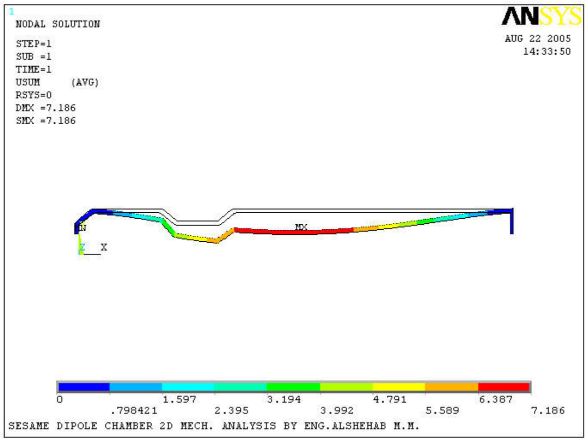

Figure 6: Deflection for 200mm anti-chamber width.

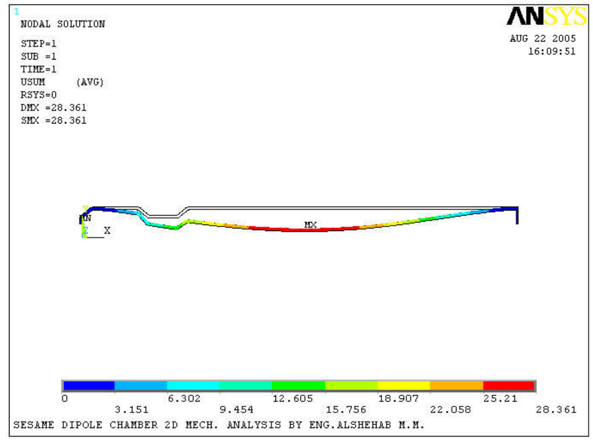

Figure 7: Deflection for 300mm anti-chamber width.

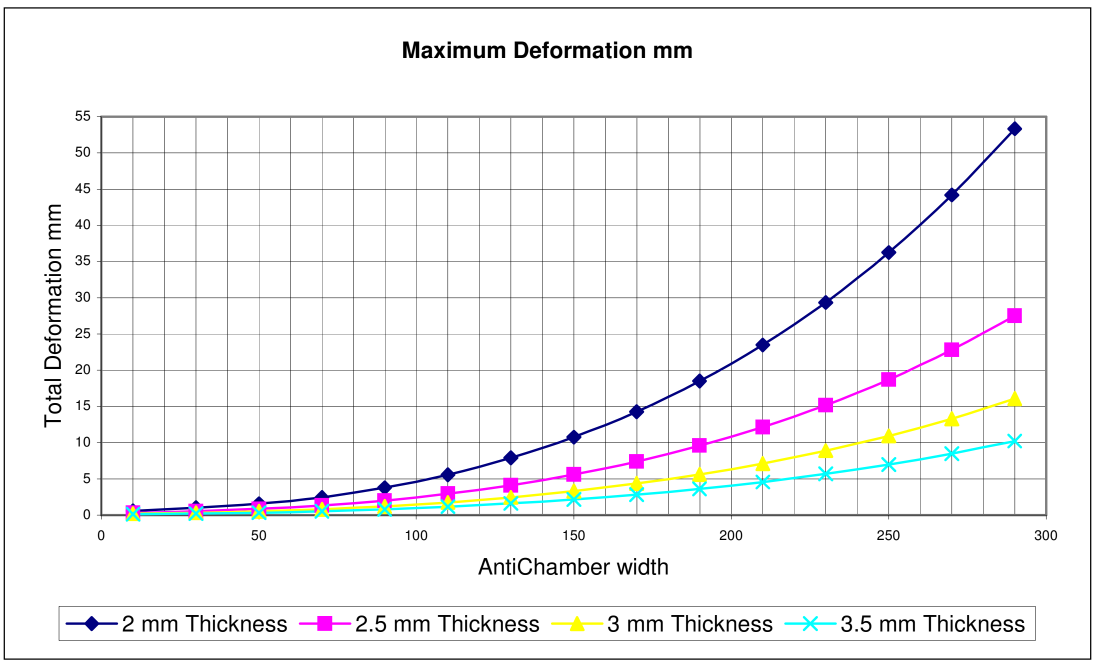

Figure 8: Chamber wall thickness effect on the max. deflection due to vacuum loading.

3.2 Self Weight load: 3D finite element analysis.

3.2.1 Results

In this section we report the finite element results for the Arc Vacuum Chamber deformation, evaluated in 3D geometry (see Fig. 1). Different supports *scenarios* were taken into consideration in this analysis.

Fig. 9÷12 show some more details of the 3D Arc vacuum chamber drawing used within the ANSYS workbench environment. Mesh contains 176226 nodes and 98995 elements; the model has a curvature/proximity value of 50.

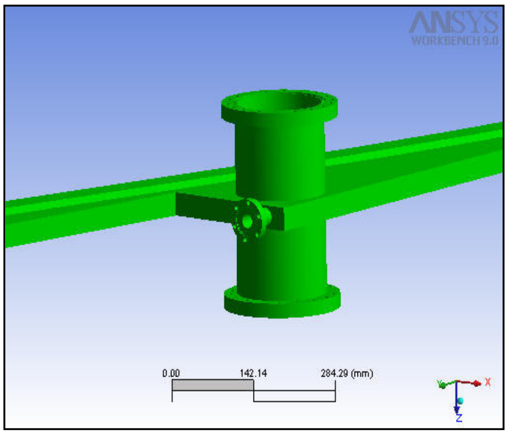

Figure 9: Zero degrees beam line.

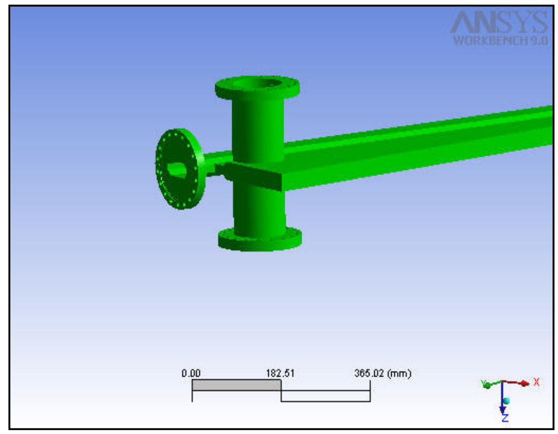

Figure 10: 4th Pumping Port.

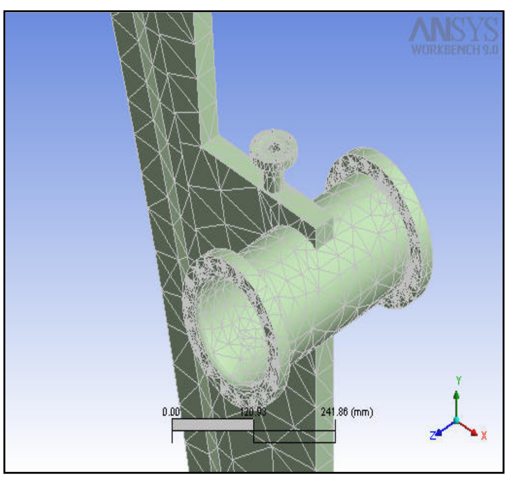

Figure 11: Meshed Model 2nd Port

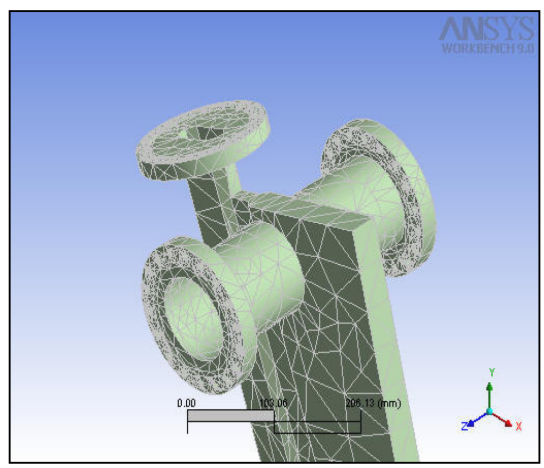

Figure 12: Meshed Model 4th Port.

We have performed deformation analysis for the following supports arrangement:

1- End flanges only.
2- End flanges and the 1st pumping port.
3- End flanges, 1st and 2nd pumping port.
4- End flanges, 1st,2nd and 3rd pumping port
5- End flanges, 1st,2nd, 3rd and 4th pumping port
6- End flanges, 1st,2nd, 3rd, 4th pumping port and 0^{o} beam line front end flange
7- End flanges, 1st, 2nd, 3rd, 4th pumping port, 0^{o} and 6.5^{o} beam lines front end flanges.

In Fig. 13÷16 the output of ANSYS of the total deformation for the first 4 cases of support arrangement are shown.

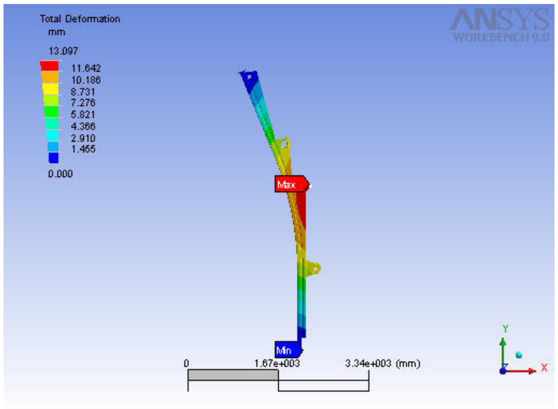

Figure 13: Total deformation for case #1

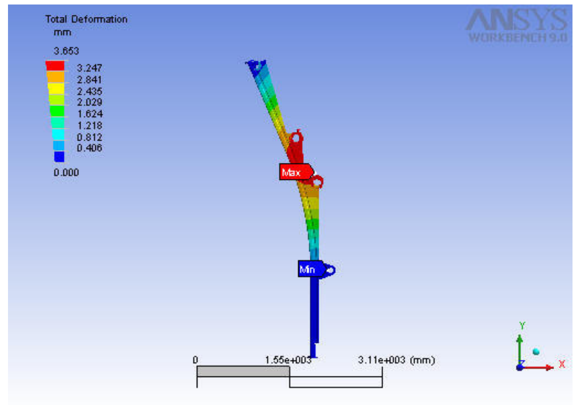

Figure 14: Total deformation for case #2

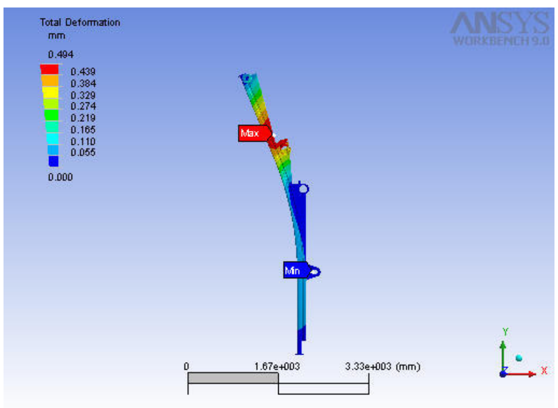

Figure 15: Total deformation for case #3

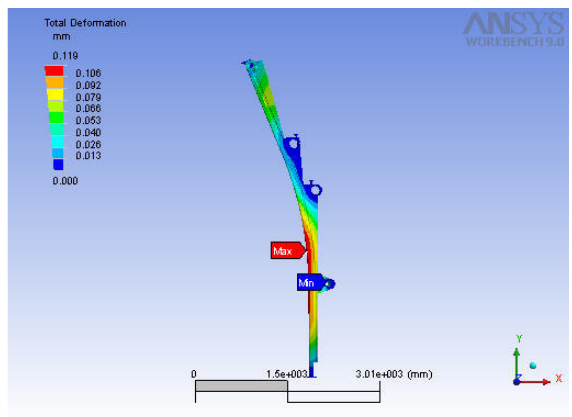

Figure 16: Total deformation for case #4

In Fig. 17 we plot the maximum deflection, while in Fig. 18 the Von-Misses stress factor and Safety factor are shown for the 7 schemes of support. Finally in Tab. 3 we summarize for the 7 support schemes the first 5 resonant frequencies.

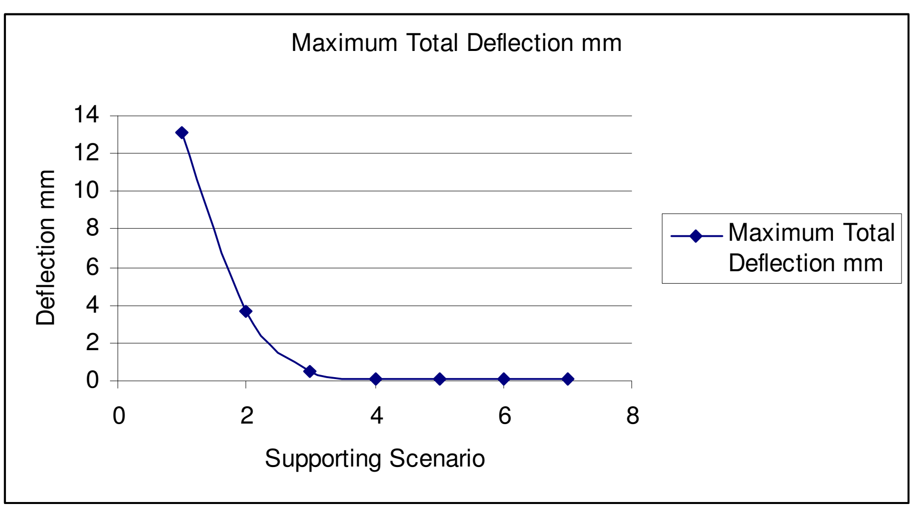

Figure 17: Maximum Total deformation vs. the 7 support schemes.

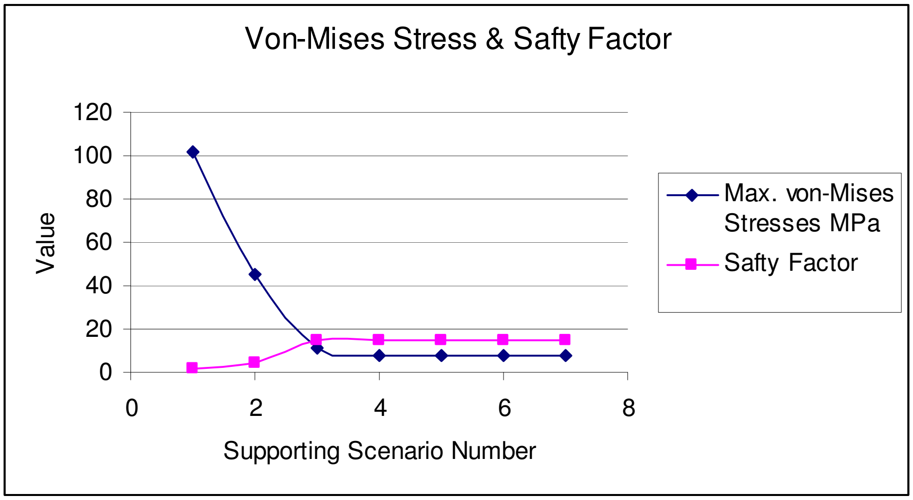

Figure 18: Von-Misses Stresses and Safety factor vs. the 7 support schemes.

Table 3: Resonant frequencies.

Supporting Scenario Number	1st Natural Frequency Hz	2nd Natural Frequency Hz	3rd Natural Frequency Hz	4th Natural Frequency Hz	5th Natural Frequency Hz
1	5.05	14.47	29.7	31.23	50.63
2	9.14	28.85	36.28	55.42	58.92
3	25.19	52.44	63.66	65.98	76.7
4	54.77	63.91	66.23	86.77	115.08
5	54.84	66.23	84.71	113.9	126.38
6	55.01	66.29	84.71	115.71	130.45
7	55.02	66.3	85.31	115.98	131.96

The maximum deformation of 13.1 mm is obviously for case # 1, where the chamber is supported only from the ends flanges. This deformation was efficiently reduced by applying the fixed support condition on the pumping port which reduces the total deflection value to about 0.12 mm (99.08%). It is also clear that there will be little gain in adding a fixed support condition at the beam front ends flanges as it could be seen from the results.

4.0 Conclusions.

The results presented in this note are the first step toward the complete understanding of all the important parameters that may affect the chamber design.
The 2D vacuum load results show that it is necessary to have ribs to support the anti chamber surface in order to decrease the chamber deformation within acceptable values (< 0.5 mm).
The 3D self-weight analysis indicates that the deformation is reduced as the number of supporting points increase, but there is no further advantage in increasing this number beyond a certain limit.
The next step toward the complete chamber design is to have a complete design analysis study regarding the ribs orientation, location, thickness and welding to the anti chamber surface. Then optimization techniques will be applied to achieve the best ribs design. In addition to more refinement to the chamber geometrical shape, pumping ports locations will be studied.

5.0 References.

[1] G. Vignola, M. Attal – SESAME Technical Note **O-1**, December 2004
[2] G. Vignola et al. - SESAME in Jordan, PAC 2005 Proceedings
[3] F. Makahleh, A. Amro – SESAME Technical Note **V-1**, August 2005
[4] ANSYS Release 9.0 Documentation, Element reference.